Journal of
Water & Climate Change

IWA PUBLISHING

Journal of Water and Climate Change Vol 13 No 11, 3883 doi: 10.2166/wcc.2022.234

Comparative analysis of long-term precipitation trends and its implication in the Modjo catchment, central Ethiopia

Kokeb Zena Besha*, Tamene Adugna Demissie and Fekadu Fufa Feyessa

Faculty of Civil and Environmental Engineering, Jimma Institute of Technology, Jimma University, Jimma, Ethiopia
*Corresponding author. E-mail: kokeb681@gmail.com

ABSTRACT

Understanding trends and variability of precipitation is essential to improve water resources utilization as well as agricultural activities. This study aims to investigate the spatiotemporal trends and variability of rainfall in the Modjo watershed, central Ethiopia. The Mann-Kendall trend (M–K) test, innovative trend analysis (ITA) and Sen's slope estimator were used to determine temporal trends, while the inverse distance weighted interpolation technique was adopted to visualize the spatial trends in time series. The result showed that complex patterns of rainfall variability that range from 16 to 59%, 18 to 63%, and 50 to 90% for the annual, summer, and spring seasons, respectively was observed over the study watershed. The result also indicated that significant trend ($p < 0.05$) in annual rainfall was detected only in 28.6% and 42.9% of the stations under the M-K test and ITA method, respectively, which indicates relatively more significant trends are displayed by the ITA method than the M–K test. At the seasonal scale, positive trends have been more dominant in the summer season ($Z > 0$, $SITA > 0$), whereas negative trends ($Z < 0$, $SITA < 0$) were detected in the spring season. Comparatively, the ITA method is found to be robust and allows more detailed trend analysis results using graphical illustrations for extreme events. The study concludes that the increasing and decreasing trends in summer and spring rainfall patterns could have implications leading to an increase in extreme events and lower agricultural productivity, respectively. The result suggests the need for planning effective adaptation strategies at the regional and local scales.

Key words: climate change, comparative analysis, Modjo catchment, trends

HIGHLIGHTS

- Comparative trend analysis approach was followed using the classical M–K test and ITA method.
- The spatiotemporal trend is analyzed at station level which is not a common approach.
- The study indicates the ITA method displays more significant trends than the M–K test.
- Increasing extreme events and lower agricultural productivity were identified as the major implications in the future.
- Establishing effective adaptation strategies in such a rain-fed agricultural watershed is needed.

GRAPHICAL ABSTRACT

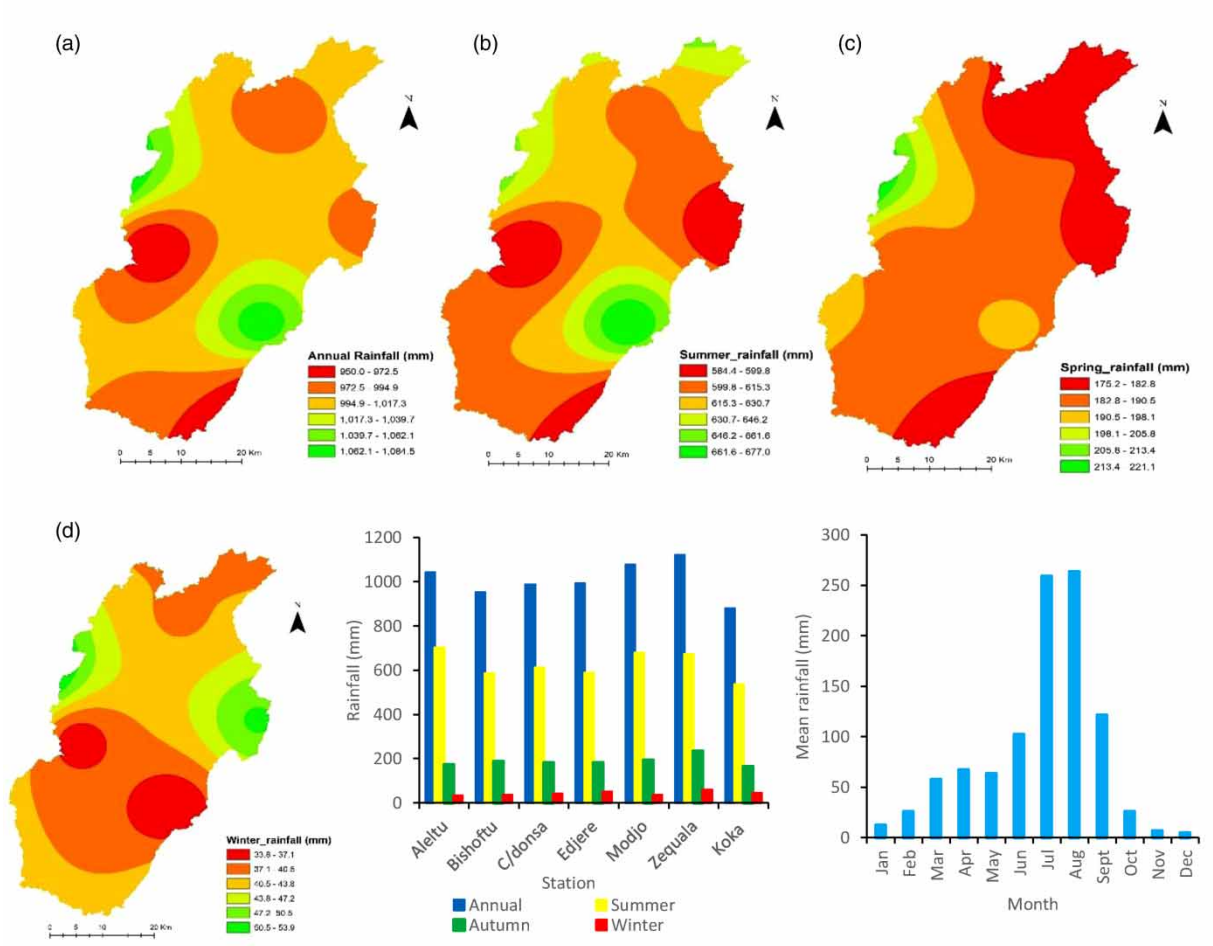

1. INTRODUCTION

The hydrologic system and water resources of a catchment are widely determined by climate change and human activities. In recent decades, climate change demands even the revision of engineering designs that affect our lives seriously (Mohammed *et al.* 2018). Precipitation is the main weather variable in which its change can be related to global warming (Li & Luo 2011), and its spatiotemporal distributions directly affect the distributions of water resources in space and time (Aziz & Burn 2005). Hence, studying the hydro-climate trends is highly important for identifying the spatiotemporal variability and management of inadequate water resources for future economic development, flood control measures as well as agricultural planning activities. Hence, a detailed analysis of rainfall trends and variability is highly important to national and local water resources management as it contributes to a better understanding of the impacts of global climate change.

In Ethiopia, precipitation is the primary source of both surface and groundwater supply, and its significant variability directly affects the quantity and quality of the water resources. Therefore, analysis and understanding of the characteristics, amount, and distribution of this variable is essential for sustainable management and to improve the utilization of water resources of the country. Various studies have been conducted regarding trends and variability in Ethiopia, with a range of spatial (e.g., national, regional) and temporal (e.g., annual, seasonal, monthly) scales (Bekele *et al.* 2017; Gummadi *et al.* 2018; Worku *et al.* 2022). However, the studies conducted in different parts of the country did not report consistent trend results even for the same areas. For example, Cheung *et al.* (2008) investigated the trends and spatial distribution of annual and seasonal rainfall over Ethiopia and reported a declining trend in the annual and summer rainfall in eastern, southern, and southwestern Ethiopia. However, Rosell & Holmer (2007) and Viste *et al.* (2013) indicated an increasing

trend result regarding the summer rainfall pattern in different parts of the country. Jury & Funk (2012) on their part reported a weak rising trend in the arid lowlands of the southeastern and a downward trend over the western highlands of the country. However, Seleshi & Camberlin (2006) found the absence of significant trends in the Kiremt (summer) and Belg (spring) seasons in many parts of Ethiopia except the eastern, southwestern, and southern parts. Recently, Worku *et al.* (2022) applied the M–K test and Sen's slope estimator to determine rainfall trends in southern Ethiopia using data for the period 1981–2018. They reported that a significant increasing trend in annual rainfall was detected in some of the stations such as Arero, Dehas, Dillo, and Miyo. Therefore, consistent rainfall trends and variability results are crucial not only for knowing the monotonic trends of an area but also for the proper estimation and analysis of water resources as well as for the planning of effective adaptation strategies.

Most of the previous trend-related studies have been conducted at the regional or basin scales (Gedefaw *et al.* 2018; Misrak *et al.* 2019; Harka *et al.* 2021) among others. However, rainfall variability and trend at the local scale or catchment level have not been given due attention and the issue was not well addressed in Ethiopia. Analyzing the spatiotemporal trends of hydroclimate variables such as rainfall is vital to look into the effects of climate change on agricultural activities as well as water resources planning and management at the catchment scale. The large-scale studies cannot be overlooked as well as not suitable to observe local variability that can affect agricultural activities, water resources, and hydrologic regimes of catchments. Moreover, the previous studies employed the conventional M–K trend test and Sen's slope estimator (SS) while quantifying the spatiotemporal trends in the country. However, these methods have limitations due to their assumptions of data distribution as well as sample size and trend calculation algorithms (Alifujiang *et al.* 2020). In addition, the classical M–K test requires the removal of the serial autocorrelation from time-series data that can alter the significant trend results (Wagesho *et al.* 2013). To overcome the stated drawback of this method, Şen (2012) developed the innovative trend analysis (ITA) method as a new statistical trend estimation approach, which is a flexible graphical method used to explore time-series trends to avoid errors when major hidden trends are detected. According to Şen (2012), the ITA method is independent of sample size, data distribution, and serial correlation. Moreover, the classical tests do not allow to identify the contribution of low and high values in the detected trend. The cited works indicated that the ITA method has some advantages compared with the conventional methods. For example, Wu & Qian (2017) applied linear regression, the M–K trend test and the ITA method to detect trends of seasonal and yearly rainfall extremes, and they concluded that the ITA method is the better one. Moreover, the ITA approach allows more detailed interpretations of trend detection, which has benefits for identifying hidden variation trends of precipitation and the graphical illustration of the trend variability of extreme events, such as 'high' and 'low' values of precipitation (Ay & Kisi 2015; Caloiero *et al.* 2018; Caloiero 2019; Alifujiang *et al.* 2020).

The objective of this study is, therefore, to analyze the spatiotemporal trends of rainfall amount of a highly agricultural catchment located in central Ethiopia by a comparative analysis of the classical M–K trend test, SS, and ITA method. The proposed study is crucial since previous studies in the region are scanty and fragmented. The nobility of the proposed study lies in the comparison between the classical M–K test and the ITA method for trend robustness. Moreover, unlike the past study in the same area (Eshetu 2020) to analyze similar issues using the classical M–K test and within the same region (e.g., Gedefaw *et al.* 2018; Misrak *et al.* 2019), this paper offers a better understanding on the distribution of annual and seasonal precipitation patterns over space and time. Finally, the study results will be helpful in identifying constraints related to climate change faced by the local farmers and provides references for further analysis of climate-related issues in an agricultural catchment.

2. STUDY AREA AND DATA USED

2.1. Description of the study area

The Modjo catchment is situated in central Ethiopia within the Awash river basin. Geographically, the catchment is located between the latitude of 8°35′00″N to 9°05′11″N and longitude of 38°54′35″E to 39°15′30″E (Figure 1). The Modjo catchment is located 70 km east of the capital city of Ethiopia-Addis Ababa and 25 km west of Adama city. The catchment is characterized by undulating topography, deep and wide valleys of small streams, and narrow flat lands at the southern part caused by poor land-use practices, soil erosion, and deposition processes. The elevation ranges between 1,566 and 3,084 m above sea level (Figure 1).

The rainfall regime of the catchment is bi-modal type, with two distinct peaks in April and August months. On the basis of recorded data of the period 1981–2020, the annual rainfall of the area varies between 846 and 1,131 mm, with maximum

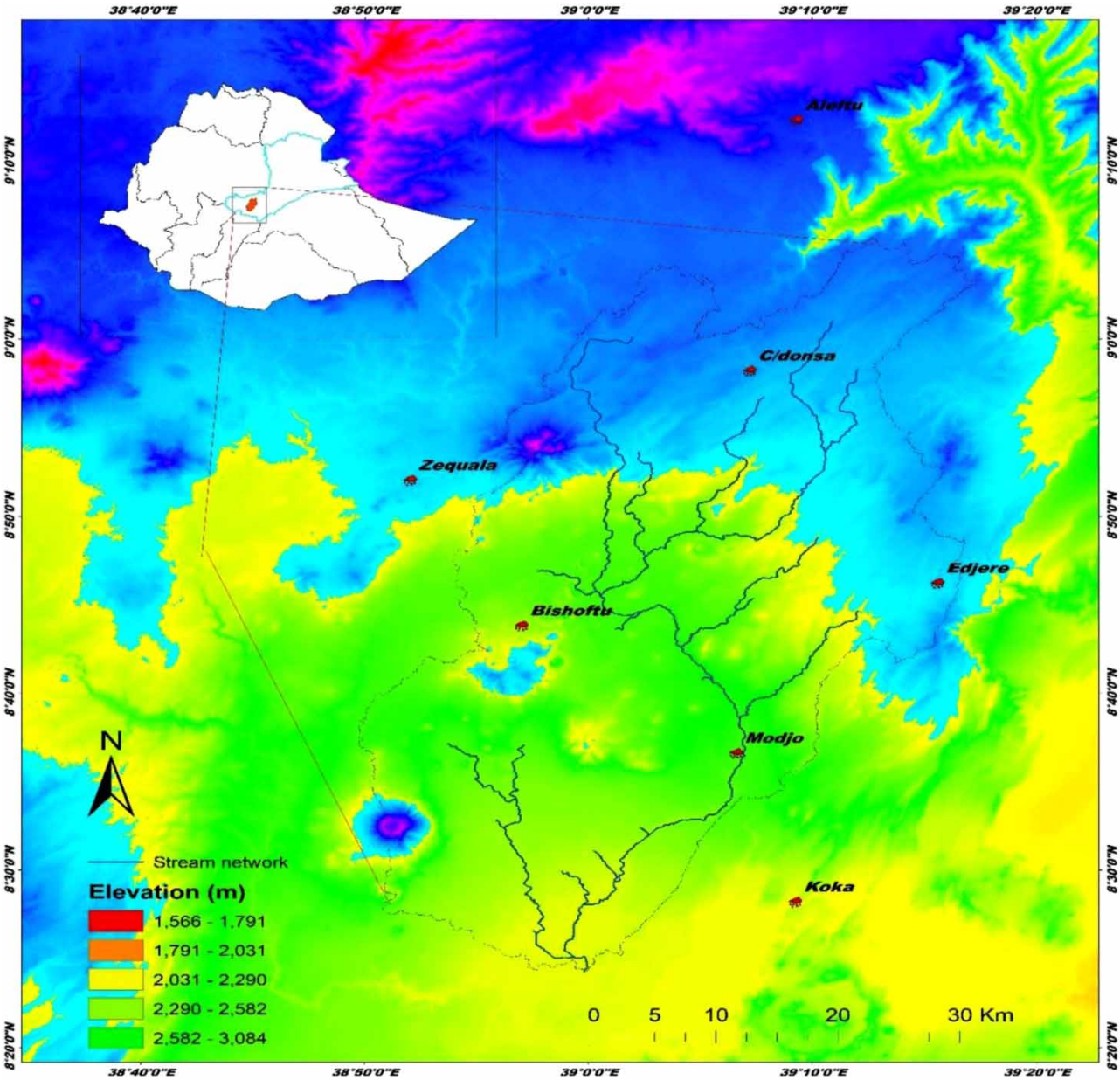

Figure 1 | Locational map of the Modjo catchment.

value in the northern and northwestern parts (https://www.ethiomet.gov.et). The rainfall that occurs during the major rainy (Kiremt) season (June to mid-September) and Belg season (March, April, May (MAM)) covers, more than 80% of total annual precipitated rainfall amounts over the catchment. Based on recent studies (Eshetu 2020), the annual mean minimum and mean maximum temperatures vary between 10.6–11.6 °C and 21–27 °C, respectively, whereas the annual average temperature of the watershed varies between 16.9 and 19.3 °C.

The natural vegetation in the catchment mostly consists of shrubs and range lands; however, Eucalyptus trees are found close to the towns and around rural villages. Agriculture is the dominant sector and source of income in the catchment. The sector is dominated by small-scale farmers those practice rain-fed mixed farming with the help of traditional technology, adopting low-input and low-output production systems. Attributable to high population growth and its pressure, most arable land area is cultivated in the catchment. In recent time, more than 90% of the catchment area is cultivated. The agro-climatic conditions make it suitable for permanent and temporary crops.

Table 1 | Geographical location of climate stations whose data records were analyzed in this study

Stations	Elevation (m)	Longitude (E)	Latitude (N)	Period	Record length (years)	% missed
Aleltu	2,663	39.155	9.206	1981–2020	40	0
Bihoftu	1,900	38.95	8.733	1981–2018	35	2.8
Chefe donsa	2,392	39.123	8.97	1981–2020	40	2.7
Edjere	2,254	39.257	8.773	1981–2018	35	2.8
Koka dam	1,618	39.154	8.469	1981–2020	40	1.4
Modjo	1,763	39.109	8.605	1981–2020	40	1.4
Zequala	3,050	38.867	8.867	1987–2020	34	0

2.2. Data used and sources

Daily precipitation datasets were collected from the National Meteorological Service Agency of Ethiopia (https://www.ethiomet.gov.et) which is used in the study to understand the spatiotemporal trends of an agricultural catchment located in the central part of the country. The data consisted of daily precipitation observations covering the period 1981–2020 from seven meteorological stations within (Bishoftu, Chefe donsa, Edjere, and Modjo) and outside (Aleltu, Koka dam, and Zequala) the catchment boundary (Figure 1). List of stations, latitude, longitude, and elevation of the meteorological stations used in the present study are presented in Table 1.

Based on the agricultural activities of the area, we divided the daily data into four seasons: summer (June–August), is the major rainy time of the catchment, autumn (March–May), is the second contributor to annual rainfall, winter (December–February), and spring (September–November). The obtained daily precipitation data were converted to average monthly and then seasonal data for the analysis of temporal trends at the station level and spatial distribution of rainfall at the catchment scale.

3. METHODS OF DATA ANALYSIS

3.1. Data quality assessment

The precipitation data were subjected to different quality control procedures such as checking missing records, homogeneity, and inconsistency tests. There are few records with continuity problems in the time-series. This may be due to instrumental failure, changing the record site, or the absence of the observer. Therefore, it is necessary to estimate and complete the missing data before using it for trend analysis. However, the choice of the methods is based on the percentage of data missed and choice of neighboring stations. When the amount of the data filled is less than 5%, linear regression can be used by identifying the relationship between the observed data of neighboring stations and that of the reference station (Aieb *et al.* 2019). In this study, the missing values were less than 3% (Table 1). Hence, linear regression was used to fill in the missing rainfall data. The other pre-processing analysis carried out was the identification of outliers, which were treated case by case using information from the date before and after the event. In the present work, the data of each station were plotted against time in days of the year format and subjected to visual examination for the presence of outliers and typing errors such as negative rainfall values.

The homogeneity tests are an important part of climate change analysis because the tests help to identify whether the variations in climate data are either due to meteorological, climatological, or external factors. Inconsistency and homogeneity of the rainfall data were checked using the Double mass curve (DMC) analysis and standard normal homogeneity test (SNHT) (Agha *et al.* 2017). By using the double mass analysis (DMA) method, cumulative annual rainfall for each station (suspect gauge) was plotted against cumulative mean annual rainfall for surrounding stations. Any deviation from the straight line would therefore mean that the data are not homogenous and inconsistent. In such a situation, a correction factor is calculated and used to correct erroneous data. The coefficient of determination (R^2) was used to show the strength of the correlation and relationship between each station and the surrounding stations and hence confirm the consistency of rainfall data. The quality control results obtained from both the SNHT and DMC tests indicate that the rainfall data are homogenous, consistent, and of good quality, and can further be used for hydrological analysis (Table 2). Moreover, the relation between the suspect gauge and the other stations was checked, and the value of the coefficient of determination (R^2) for the stations is large indicating

Table 2 | Summary of homogeneity and autocorrelation tests for annual precipitation of the stations

	SNHT homogeneity test		DMA		Auto correlation check	
Station	Homogeneous	Inhomogeneous	Homogeneous	Inhomogeneous	Accepted	Rejected
Aleltu	✓		✓		✓	
Bihoftu	✓		✓		✓	
Chefe donsa	✓		✓		✓	
Edjere	✓		✓		✓	
Koka dam	✓		✓		✓	
Modjo	✓		✓			✓
Zequala	✓		✓		✓	

the strong linear relationship between each station and other surrounding stations. Therefore, the identification of trend tests and their magnitudes was carried out on the homogenous rainfall data collected from the seven stations.

3.2. Analysis of rainfall variability and serial correlation

3.2.1. Rainfall variability analysis

The coefficient of variation (CV) was used to evaluate the rainfall variability of the study catchment. CV measures the relative dispersion of time-series data from the mean. It can be estimated from the ratio of standard deviation (SD) to mean rainfall values. Overall, in using the CV, the degree of rainfall variability can be analyzed based on the following: if $CV < 20$ (low variability), if $20 < CV < 30$ (moderately variable), high when $30\% < CV < 40\%$, very high when $40\% < CV < 70\%$, and extremely high when $CV > 70\%$ (Asfaw *et al.* 2018). Therefore, the CV was applied to understand the variability of annual and seasonal rainfalls in our study area.

3.2.2. Serial correlation

Tests for serial correlation are highly important to avoid autocorrelation effects from 1 year to the next year, particularly for the application of the classical M–K test (Yue & Wang 2002). Autocorrelation is one of the significant problems that introduce uncertainties and errors during trend detection. In the present work, removing the autocorrelation effects was checked using the following equation:

$$r_1 = \frac{(1/n) - \sum_{i=1}^{n-1} (X_i - X_a)(X_{i+1} - X_a)}{(1/n) \sum_{i=1}^{n} (X_i - X_a)^2} \quad (1)$$

Here, r_1, X_i, Xa, and n represents the correlation coefficient at lag 1, precipitation time-series, the mean value of precipitation, and the number of observations in the time-series, respectively. r_1 was computed at a 5% confidence interval using the following equation:

$$r_1(5\%) = \frac{-1 \pm 1.96\sqrt{n-1}}{n-1} \quad (2)$$

It is important to note out that if the r_1 value falls within the confidence limits, there is no significant autocorrelation in the dataset and the M–K test can be applied on the dataset to examine the trend. On the contrary, if r_1 falls outside of the confidence interval, it can be said that the time-series exhibits a significant autocorrelation and the M–K test should be applied after the removal of the autocorrelation (Alashan 2020). Based on the result (Table 2), except rainfall record at the Modjo station all the stations have no correlations at the 5% level. The annual rainfall of the Modjo station is dependent at a 5% significant level and the significant autocorrelation was removed as per the suggested correction procedure for this particular

station before using the data for trend analysis by the M–K test. The summary of the autocorrelation test results at the station level is presented in Table 2.

3.3. Analysis of temporal trends in annual and seasonal rainfall

3.3.1. ITA method

In the study, the ITA method, developed by Şen (2012), with later mathematical and graphical improvements (Şen 2017; Alashan 2018) was applied to detect the trends in rainfall time-series. The ITA method is chosen taking the advantage of its freeness from different types of assumptions and its applicability both for graphical and statistical trend analysis. The technique was used in different parts and proved as an effective method of trend analysis (Gedefaw *et al.* 2018; Malik *et al.* 2019). In the process, initially, the time-series is separated into two equal parts and arranged in ascending order. The first part of the time-series (X_i: $i = 1, 2, 3, \ldots, n/2$) is placed on horizontal x-axis and the other time-series (X_j: $j = n/2 + 1, n/2 + 2, \ldots, n$) is located on the vertical y-axis on the Cartesian coordinate system. Graphically, the ITA method provides visions in trend analysis, namely monotonic/non-monotonic increasing, monotonic/non-monotonic decreasing, and trendless conditions (Oztopal & Şen 2017). A monotonically increasing/decreasing trend can be detected if all points are distributed above/below the 45° (1:1 line), respectively; a non-monotonically increasing/or decreasing trend is when most of the points are distributed above/or below the 45° line; a monotonically decreasing trend can be detected if all points found below the 45° line; a non-monotonically decreasing trend can be detected if most of the points are below the 45° line, and a trendless condition is when the points are concentrated on the 45° line (Şen 2012).

The slope parameter of the ITA method is the stochastic property as a function of the sample means of the first-half (n_1) and the second-half (n_2) time-series of arithmetic mean rainfall data values. In the study, the sub-series data lengths are equal ($n_1 = n_2$), showing that each of the distribution points has equal probability values (i.e., $1/n_1 = 1/n_2$). According to Şen (2017), the straight-line trend slope (S_{ITA}) can be estimated using the following expression:

$$S_{ITA} = \frac{2x(y_j - x_i)}{n} \tag{3}$$

where S_{ITA} stands for the ITA slope parameter, n is the total number of observations, x_i and y_j are the arithmetic mean of the first and the second half of the sub-series, respectively. Because x_i and x_j are also stochastic variables, the expectation $E(S_{ITA})$ of the slope can be calculated using Equation (4), by considering the expectations of both the first- and second-half time-series sides (Harka *et al.* 2021):

$$E(S_{ITA}) = \frac{2}{n}[E(y_j) - E(x_i)] \tag{4}$$

For the no trend condition, $E(y_j) = E(x_i)$, then, $E(S_{ITA}) = 0$ and SD of the two half time-series ($\sigma_x = \sigma_y = \sigma/\sqrt{n}$), σ is the SD is of the parent series. If $E(y_j) \neq E(x_i)$, the difference between $E(y_j)$ and $E(x_i)$ gives the variance (Equation (5)) and the SD of the slope (Equation (6)):

$$\sigma^2_{S_{ITA}} = \frac{8}{n^2}[E(y_j) - E(y_j x_i)] \tag{5}$$

$$\sigma_{S_{ITA}} = \frac{2\sqrt{2}}{n\sqrt{n}}\sigma\sqrt{1 - \rho y_j x_i} \tag{6}$$

In the stochastic processes, the term $\rho y_j x_i$ is the correlation coefficient between the two mean values, and can be estimated using Equation (8):

$$\rho y_j x_i = \frac{E(x_i y_j) - E(x_i)E(y_j)}{\sigma x_i \sigma y_j} \tag{7}$$

In the end, the upper and lower confidence limit (CL) of the trend slope was calculated according to Equation (8) (Şen 2015):

$$CL_{(1-\alpha)} = 0 \pm S_{crt} x \sigma_{S_{ITA}} \tag{8}$$

Here, S_{crt} represents the critical slope for standardized time-series at ± 1.96 for a 95% significant level ($S_{crt} = 0 \pm 1.96 x \sigma_{S_{ITA}}$). If the ITA slope ($S_{ITA}$) value falls outside of the lower and upper CL values, then the null hypothesis of no significant trend is to be rejected at α significance level (Şen 2015). In a two-sided condition, the null hypothesis (H_0) indicates that no trend in time-series data, and the alternate hypothesis (H_1) describes that there is a trend in time-series data at $\alpha = 5\%$ with $Z = \pm 1.96$. If $\pm S_{ITA} > \pm \mathrm{CL}_{(1-\alpha)}$, then H_0 is rejected and H_1 is accepted. The positive and negative value of S_{ITA} indicates a rising and falling trend in the time-series data, respectively. The positive and negative value of S_{ITA} indicates an increasing and decreasing of trend in time-series data, respectively (Şen 2017).

3.3.2. M–K trend test

The M–K trend test is one of the frequently used statistical tests to detect monotonic (increase/or decrease) trends in hydro-climatological time-series (Worku *et al.* 2019; Yimer *et al.* 2020). The M–K test (Mann 1945; Kendall 1975) is a nonparametric approach, which searches for a trend in time-series without specifying whether the trend is linear or non-linear. In this work, we used this test and compared it with that of the ITA method. The test statistics (S) is defined using the following expression:

$$S = \sum_{k=1}^{n-1} \sum_{j=k+1}^{n} \sin(x_j - x_k) \tag{9}$$

where x_j and x_k are time-series in the years i and j ($j > k$) and n-length of the time-series. An increasing trend is noticed if the value of S is positive and if it is negative, a decreasing trend in the data series. The sign function is given as:

$$\mathrm{Sgn}(x_j - x_k) = \begin{cases} 1, & \text{if } x_j > x_k \\ 0, & \text{if } x_j = x_k \\ -1, & \text{if } x_j < x_k \end{cases} \tag{10}$$

Taking m as the number of tied groups, with tied observations, $V(S)$ is the variance and S is the Kendall sum statistic, j and k are the years, and n as the length of data (years) for a time-series. The variance can be estimated as follows:

$$V(S) = \frac{n(n-1)(2n+5) - \sum_{i=1}^{m} t(t-1)(2t+5)}{18} \tag{11}$$

The difference ($x_j - x_k$), when $j > k$, represents a function (indicator) which exhibits 1, 0, or -1 (values). The standard normal Z value is taken into consideration to identify the monotonic trend, which is given by,

$$Z = \begin{cases} \dfrac{S-1}{\sqrt{V(S)}} & \text{if } S > 0 \\ 0 \quad \text{if } S = 0 \\ \dfrac{S+1}{\sqrt{V(S)}} & \text{if } S < 0 \end{cases} \tag{12}$$

For the presence of a significant trend, the calculated Z value is compared with standard normal distribution with two-tailed significance levels. In this study, the null hypothesis should be accepted at $\alpha = 5\%$ level of significance. Moreover, an increasing (upward) trend should be interpreted if $Z > 0$ or the time-series experiences a decreasing (downward) trend if $Z < 0$, where as if $Z = 0$, a trend due to random fluctuation, both increase and decrease trends have similar impacts, hence entirely there is no trend in the time-series.

3.3.3. Sen's slope estimator

It is apparent that the M–K trend test is unable to estimate magnitude of trend changes. For this purpose, the SS (Şen 1968) was applied in this study to determine the magnitude of trends. For two data point, the magnitude of the SS slope line (Q_j), the median of the slope (β) and percentage of trend (Tp) can be estimated using Equations (13)–(15), respectively.

$$Q_i = \frac{x_j - x_k}{j - k} \quad \text{for } i = 1, 2, \ldots, N \tag{13}$$

$$\beta = \begin{cases} Q\left[\frac{(N+1)}{2}\right] \\ Q\left[\frac{N}{2} + Q\frac{(N+2)/2}{2}\right] \end{cases} \tag{14}$$

$$T_p = \frac{\beta}{\pi_{ave}} \times 100 \tag{15}$$

where x denotes the data point, n is the number of data, π_{ave} is the average values over the period of record, j and k are the corresponding times. If the estimated β value is positive, an increasing trend, otherwise, a decreasing trend.

3.4. Spatial variability of rainfall

In Ethiopia, ground stations have missing values and leading to inconsistent, and more discrete and unreliable datasets for trend analysis. This requests for the use of data reconstruction through interpolation methods. Therefore, the measured rainfall amount from the available ground locations is weighted spatially using deterministic interpolation techniques. For this purpose, the inverse distance weighted interpolation (IDW) method was applied to spatially interpolate the rainfall time-series data. This method is a deterministic interpolation technique because it is directly based on the surrounding measured values, which works based on the assumption that the interpolating surface should be influenced most by nearby points and less by more distant points (Pingale *et al.* 2014). The IDW weights the points closer to the prediction location greater than those farther away. The following IDW interpolation formulas were applied to create rainfall maps at the annual and seasonal scales:

$$Z(\text{Lo}) = \sum_{i=1}^{N} \lambda_i Z(\text{Li}) \tag{16}$$

$$\lambda_i = \frac{d_{io}^{-P}}{\sum_{i=1}^{N} d_{io}^{-P}} \tag{17}$$

where Z(Lo) is the prediction value for location Lo, N is the number of measured values points surrounding the prediction location, λ_i is unknown weight to the measured value at the ith location, Z(Li) is the measured value at the ith location, and p is power parameter, which can be any real number greater than 0. A higher power results in less influence from distant points. A large p results in nearby points wielding a much greater influence on the unconsidered location than a point further away resulting in an interpolated output (Hussain *et al.* 2021). To minimize the interpolation errors, the power parameter $(p) = 1$ was adopted at the annual and seasonal time scales to have more detailed output surface and to ensure a high degree of local influence. The spatial variability and distributions of seasonal and annual rainfall data were analyzed using Arc GIS 10.4 software.

4. RESULTS AND DISCUSSION

4.1. Analysis of annual and seasonal rainfall variability

The rainfall characteristics and contributions of seasonal rainfalls at the station level were computed for the period 1981–2020. Figure 2 displays the average annual and seasonal rainfall distribution at each station. The observed precipitation analysis from 1981 to 2020 indicates that the Modjo catchment received mean annual precipitation between 8,496 and 1,187 mm, with a SD of 143.7–306.2 mm/year (Table 3). The seasonal distribution of average rainfall showed that summer and winter

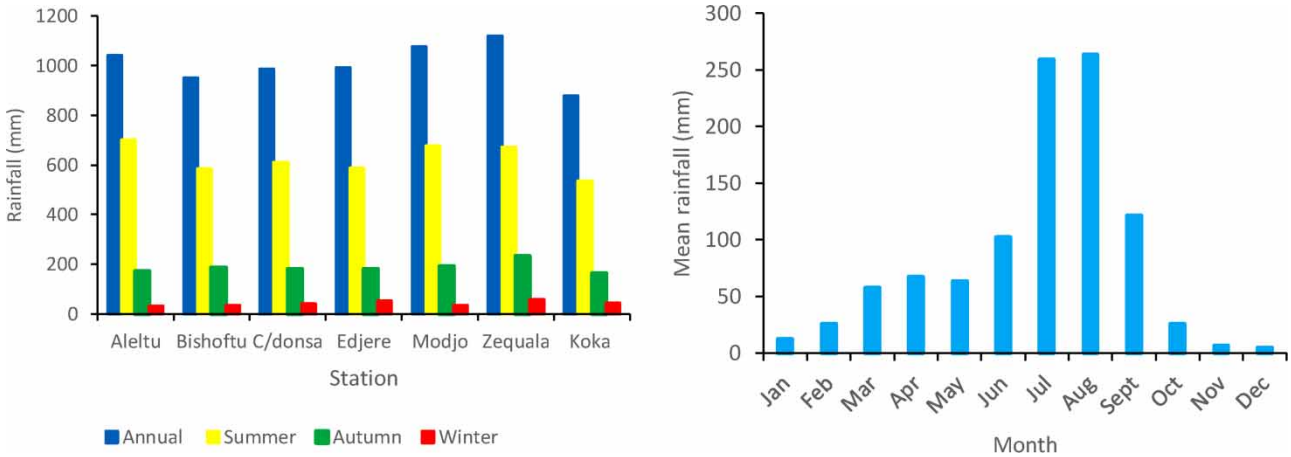

Figure 2 | Station level annual and seasonal mean rainfall and monthly rainfall at catchment scale (1981–2020).

contributed the maximum and minimum rainfall amounts (62 and 4.2%, respectively) over the study catchment. August received maximum average rainfall (263.2 mm), and minimum average rainfall was recorded during the month of December (4.6 mm) (Figure 2). Seasonally, point rainfall during the major rainy season (summer) was the highest at Aleltu (67.4%) and the lowest at the Edjere (59.3%) station (Table 3). The summer season (JJA) rainfall varies between 519 and 742 mm, with some high coefficient variabilities. The major share of the annual rainfall was from the summer season (JJA) and spring (MAM), which varies from 55 to 70% and 16 to 23%, respectively. The wet season rainfall precipitated over the catchment is crucial for water resources and agricultural activities.

The annual and seasonal precipitation variability was assessed using the CV. The CV is a statistical measure of dispersion around the mean, which is the ratio of SD to the mean. Areas with high annual precipitation showed less inter-annual variation, whereas areas with low annual rainfall experienced high inter-annual variation. The annual precipitation distribution of the catchment showed from low (CV < 20%) to moderate (i.e., 20% < CV < 30%) variability, except at the Koka dam station which shows a very high variability (i.e., 40% < CV < 70%) in annual precipitation (Table 3). With regard to the seasonal rainfall, low to high variability was observed in all seasons (Table 3). For example, the CV value for summer (18–58%), winter (4 to >119%), and spring (32 to >77%). During the winter season, CV is greater than 50% in most stations except at Bishoftu and Chefe donsa, but this is not a crop season and has no significant impact on the cropping system in the area. Generally, summer and spring seasons rainfall patterns are highly variable over the area, which could affect the agricultural productivity and water resource sustainability over the catchment. Moreover, the high rainfall variability during the spring season can be an indication of low agricultural production in such highly populated area of the country. Comparatively, the seasonal rainfall

Table 3 | Statistical summary of annual and seasonal rainfall characteristics of the Modjo catchment (1981–2020)

	Annual rainfall		Summer season		Winter season		Spring season	
Station	***P* (mm)**	**CV**	***P* (mm)**	**CV**	***P* (mm)**	**CV**	***P* (mm)**	**CV**
Aleltu[a]	1,054.2	16.5	741.8	21.6	29.1	84.4	175.9	52.8
Bihoftu	849.6	17.0	519.1	20.9	26.8	4.5	151.5	54.1
Chefe donsa	925.3	19.4	590.6	18.4	34.4	4.3	155.0	59.8
Edjere	881.5	16.7	527.4	22.5	42.2	96.0	152.8	50.6
Koka[a]	869.4	55.9	522.4	57.9	39.1	119.3	165.9	67.4
Modjo	981.9	22.8	621.2	28.4	32.1	115.4	178.9	57.9
Zequala[a]	1,187.1	27.1	649.8	26.7	55.1	104	274.8	69.1

P, annual/seasonal mean point rainfall; CV, coefficient of variations (%).
[a]Stations located outside the study catchment.

of the catchment showed more variation than that of the annual variation of the period. The finding of this study is in line with the studies recently carried out in the area (Bekele *et al.* 2017; Gedefaw *et al.* 2018; Mahtsente *et al.* 2019; Eshetu 2020; Bayable *et al.* 2021). The highest seasonal rainfall variability was observed during winter time, which varies from 4.5 to 119 over the catchment. Previous studies by Degefu & Bewket (2014), Asfaw *et al.* (2018), and Mekonen & Berlie (2020) indicated that the winter season rainfall is highly variable in Ethiopia.

4.2. Spatial distribution and variability of rainfall

The spatial variability of rainfall patterns is very important for impact assessment and adaptation planning for extreme events such as floods and droughts (Malik *et al.* 2019). The annual, summer, spring, and winter seasons precipitation amount of the Modjo catchment was spatialized by the inverse distance weight interpolation method to identify the portion of the catchment that exhibits low and high precipitation distribution. Figure 3 shows the spatial distribution and variability of annual and seasonal precipitation amounts over the study area. As can be observed, the annual precipitation on the catchment is unevenly distributed, with more precipitation in the west and less precipitation in the east and southern parts (Figure 3(a)). In the catchment, mainly the high-altitude areas received more rainfall than the low-altitude areas. The northern and parts of the western regions received the highest annual rainfall of the period that ranges from 1,065 to 1,085 mm (Figure 3(a)). The lowest annual rainfall was observed in the eastern, southwestern, and parts of the northern regions of the watershed, which had annual rainfall of the time between 950 and 970 mm (Figure 3(a)).

Figure 3(b) presents the spatial distribution and its variability of the summer season precipitation over the Modjo catchment. The summer season precipitation followed almost the same spatial distribution as that of the annual, except for some changes in the central parts (Figure 3(b)). During this season, the highest rainfall values were recorded in the western (which has the highest topography in the catchment), southeastern, and small parts of the northern region while the lowest rainfall values of the period were recorded in the southeastern, eastern and northwestern parts of the catchment (Figure 3(b)). This may have an impact on the agricultural productivity of the area as the area is one of the main farming of cereal crops. Figure 3(c) depicts the spatial distribution of rainfall during the autumn season (MAM) rainfall distribution of the period. The autumn (MAM) season is the second contributor of annual rainfall amounts. This season follows partially similar trends as that of the summer season. As can be seen, the spatial rainfall distribution in the western parts of the catchment received relatively better rainfall amounts, while the northern and southern, and northeastern parts received the lowest rainfall amount (Figure 3(c)). During this season, the highest rainfall values were observed in the western region, which ranges from 213–221 mm, whereas the rest parts of the catchment experienced a very low rainfall amount throughout the year. Winter (December, January, February (DJF)) is the season with the smallest rainfall amounts in the region (Figure 3(d)). This season is usually used for planning and preparation for the next cultivation season.

Many studies have been conducted to analyze the spatial variability of precipitation in different parts of the country (e.g., Wagesho *et al.* 2013; Alemu & Bawoke 2019; Harka *et al.* 2021) are among others. Spatially, the annual and seasonal rainfall variabilities were assessed by Worku *et al.* (2022) in the south central Ethiopia, and a decrease from the northeast and northwest parts of their study area. Fitsum *et al.* (2017) stated the spatial distribution of rainfall in Ethiopia is radically influenced by complex topography and elevation as the major controls of climate in the country.

4.3. Temporal trends of annual and seasonal rainfall

4.3.1. Trends of annual rainfall

In this study, comparative approaches of the classical and ITA methods were employed to examine the long-term rainfall trends of the Modjo catchment. SS is also considered to estimate trend magnitude. The annual trend analysis result under different methods is presented in Table 4. As per the M–K test, non-significant trends were dominant in the annual precipitation except at Zequala stations (Table 4), which revealed decreasing trend ($Z = -3.13$, $p < 0.05$) (Table 4). Thus, the decreasing significant trend at these stations could be attributed to climatic variability. All the other increasing and decreasing trends were not significant in statistical terms. However, increasing trend tendencies were dominant in the catchment. There is an increasing trend ($Z = 1.90 \geq 1.65$ and $p = 0.065 < 0.10$) in the Modjo station according to the M–K test, but there is no trend according to these tests at a 95% significant level. Generally speaking, it was observed that the annual rainfall in high-altitude stations shows decreasing trend and the opposite is true for the low-altitude stations considered in the study area (Table 4). Similarly, the magnitudes of positive and negative SS are recorded in five and two stations, respectively

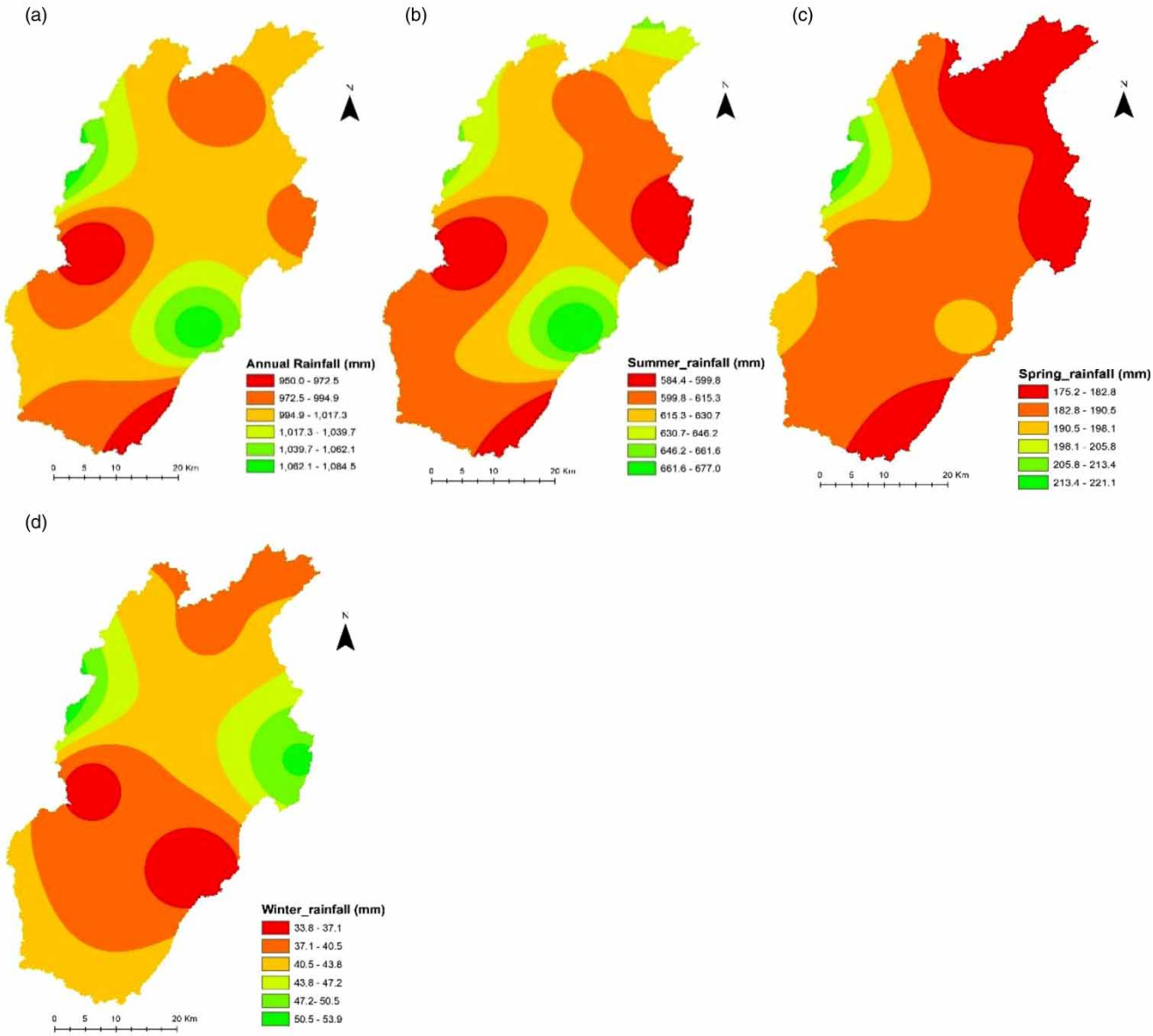

Figure 3 | Spatial distribution and variability of annual and seasonal rainfall (1981–2020).

(Table 4.) The SS value was maximum in the Koka dam (+6.28 mm/year) and the minimum trend magnitude was obtained in Zequala (−18.54 mm/year) stations (Table 4).

The statistical and graphical approaches of the ITA method have also been applied in order to show the robustness of trends in the study catchment. In this work, the significance level ($\alpha = 5\%$) was considered to measure the significance or non-significance of the rainfall trends on multiple scales. If the computed value of S_{ITA} is less than the critical value (S_{crt}), then the detected trend is a non-significant trend at a 5% significance level. According to the ITA method, there has been an increasing or decreasing trend in most of the stations as the S_{crt} value is outside the lower/upper CL in most of the stations Except at Aleltu and Zequala stations, the annual rainfall trends at the remaining stations were found to be insignificant at 5% level of significance under the ITA method (Table 4). The annual rainfall trend at Aleltu and Zequala stations showed a statistically significant decreasing rate of 3.74 and 13.98 mm/year, respectively, at a 5% significance level compared with the computed critical slope (S_{crt}) 1.063 and 1.706 mm/year in that order (Table 4). From the ITA analysis result, the rainfall trend of Modjo and Zequala stations showed maximum increment and decrement rates, with ITA slope of 8.05

Table 4 | Summary of annual precipitation trend results using different methods

	M–K test				ITA method			
Station	***Z***	***p*-value**	**Trend type**	***Q* (mm/year)**	S_{crt} **(at** $\alpha = 5\%$**)**	S_{ITA}	$CL_{(1-\alpha)}$	**Trend type**
Alelru	−1.20	0.340	yes ↓	−2.95	−1.063	−3.74	± 0.5766	yes ↓ *
Bishoftu	0.47	0.6412	yes ↑	0.780	0.6488	0.922	±0.2148	yes ↑
Chefe donsa	0.20	0.4287	yes ↑	0.210	0.5405	1.18	±0.1491	yes ↑
Edjere	0.68	0.5009	yes ↑	1.40	0.8321	4.60	±0.3533	yes ↑
Koka	1.12	0.2697	yes ↑	6.28	−2.735	−1.52	±4.245	yes ↓
Modjo	1.90	0.0650	yes ↑	5.10	1.365	8.05	±0.951	yes ↑
Zequala	−3.13	0.0002	yes ↓*	−18.54	−1.706	−13.98	±1.485	yes ↓ *

Z, M–K trend test statistics; *Q*, Sen's trend slope value; S_{ITA}, ITA trend slope value, S_{crt}, critical slope.
*Significant trend at 0.05 level.

and −13.98 mm/year, respectively. In general, similar increasing and decreasing trend results have been detected by the ITA method except for the Koka station, which showed a significant decreasing trend under the ITA method (Table 4).

In Figure 4, the innovative scatter of points is presented to indicate whether there is a trend or not in the time-series. From the plots, one can view the trend tendency as monotonic positive/or negative trends, non-monotonic positive/or negative trends, and trendless conditions depending on the position of the scatter points. With regards to the annual rainfall, a monotonic negative trend has been clearly evidenced for the Zequala station, while Edjere records increasing monotonic trends (Figure 4). Non-monotonic positive trends were detected for Bishoftu and Koka dam, whereas Chefe donsa records decreasing non-monotonic trends. On the other hand, trendless time-series were recorded for Aleltu, and Bishoftu stations in the period (Figure 4).

The results obtained in this study agree with the findings of other papers. For example, the study on spatiotemporal variability in rainfall conducted by Arragaw & Woldeamlak (2017) indicated that annual rainfall pattern increases insignificantly in the central parts of Ethiopia. The findings of the result are also in agreement with that of Alemu & Bawoke (2019) who reported that the annual rainfall showed an insignificant rising trend in Ethiopian highland areas. In the study by Harka *et al.* (2021), most of the rainfall stations in the southern Rift Valley of Ethiopia showed an increasing trend in annual time scale. Contrary to our finding, some studies in the region (e.g., Mahtsente *et al.* 2019; Gebremichael *et al.* 2022) reported in their work that insignificant decreasing trends in the annual rainfall for the stations in common (i.e., Koka dam and Modjo stations). However, Eshetu (2020) analyzed the temporal trends in the same catchment during the past 30 years (1981–2010), and concluded that the annual precipitation shows the statistically insignificant trend for all of the stations under the M–K test. But in this work, based on the longer precipitation time-series, even though insignificant increasing trends are dominant over the catchment, a statistically increasing trend was also identified for the station in common (i.e., Edjere station) at the 5% significant level (Table 4). This difference may be due to the time period considered in our case as well as the quality control processes we followed.

4.3.2. Trend of seasonal rainfall

Based on the agricultural activities of the area, a year is divided into four seasons, namely autumn, summer, spring, and winter (Mohammed *et al.* 2018). The spring season extends from March to May, the short rainy season (locally known as Belg); the summer season rainfall ranges from June to mid-September, (locally called as Kiremt), the period in which the main agricultural activity is conducted. The winter season has 3 months in Ethiopia (December, January and February) whereas the autumn season includes September, October, and November months. The summer, spring and winter seasons are rainy seasons in Ethiopia in general and in our study area in particular. Therefore, we considered the rainfall variation and trends for these seasons, and the autumn season does not contribute a significant amount of rainfall, hence is not considered in this work.

At the seasonal scale, upward trends were dominantly occurring in four of the seven stations during the summer season (Table 5). Under the M–K test, only two of the stations (Modjo and Zequala) show a significant increasing/decreasing trend. However, under the ITA test, a significant downward trend was detected only at Bishoftu ($S_{ITA} = -0.35$ mm/year)

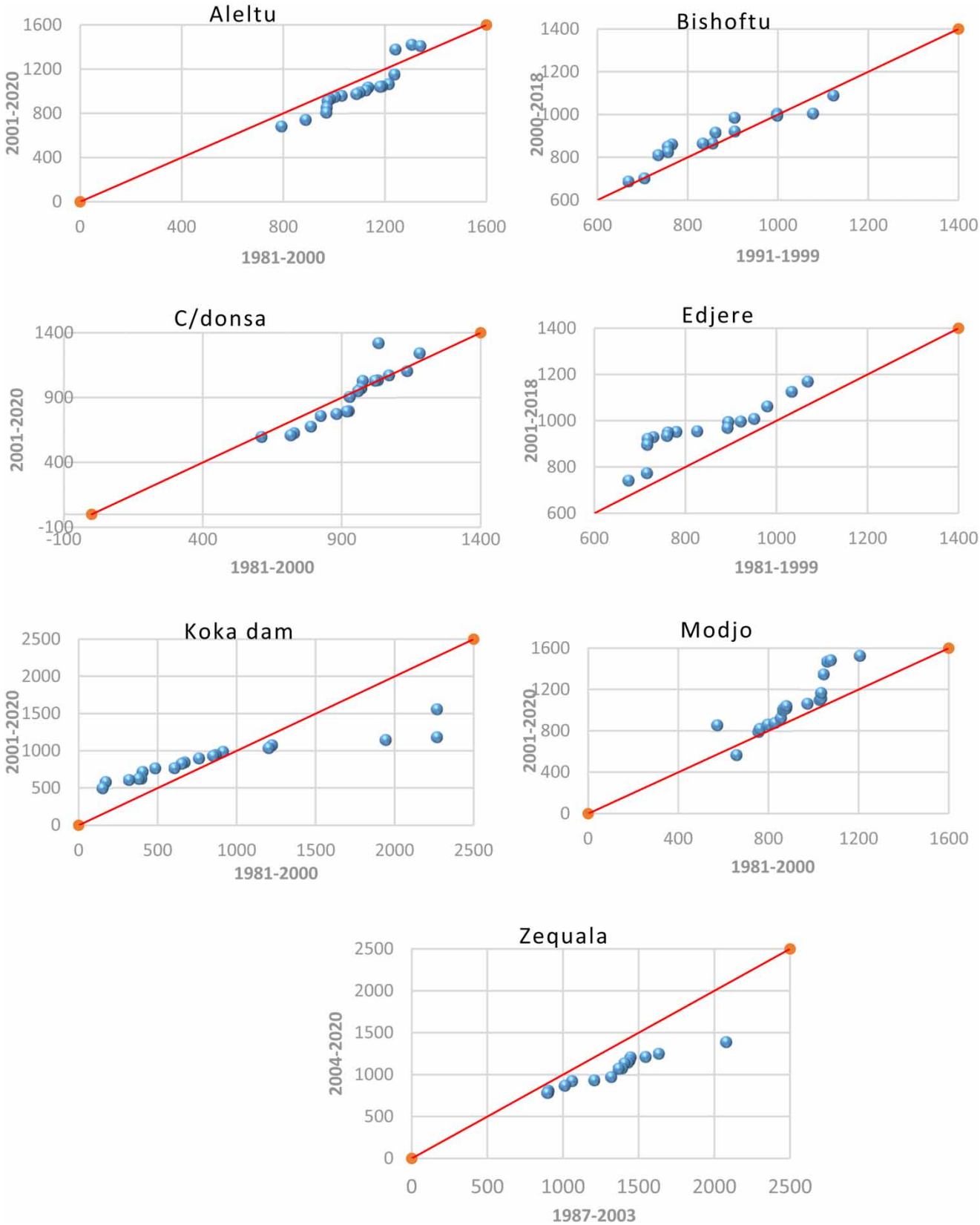

Figure 4 | ITA scatter plots of annual rainfall at the station level.

Table 5 | Results of seasonal precipitation trends between 1981 and 2020

Seasons			Aleltu	Bishoftu	Chefe donsa	Edjere	Koka	Modjo	Zequala
Summer	Jun-Aug								
		S_{crt} ($\alpha = 5\%$)	0.9329	−0.0675	−2.66	2.72	1.160	1.132	−1.949
		S_{ITA}	2.67	−0.35	−0.1747	4.88	1.63	6.49	−10.35
		$CL_{(1-\alpha)}$	±0.4440	±0.00232	±3.602	±3.78	±0.6868	±0.6533	±1.937
		Trend	yes ↑	yes ↓*	yes ↓	yes ↑	yes ↑	yes ↑	yes ↓*
		Z	1.53	−0.06	−1.03	1.26	1.38	2.92	−3.25
		p-value	0.1343	0.2962	0.051	0.2153	0.1757	0.006	0.0002
		Q (mm/year)	4.14	−0.056	−1.745	1.84	6.045	6.76	−12.60
		Trend	yes ↑	yes ↓	yes ↓	yes ↑	yes ↑	yes ↑*	yes ↓*
Winter	Dec-Feb								
		S_{crt} ($\alpha = 5\%$)	−0.4641	−0.1884	−0.2577	−0.2716	−0.186	−0.2452	−0.4579
		S_{ITA}	−0.8677	−0.46	−1.036	−0.70	−1.25	−0.400	−3.51
		$CL_{(1-\alpha)}$	±0.0295	±0.0181	±0.0339	±0.0376	±0.0177	±0.0307	±0.107
		Trend	yes ↓*	yes ↓*	yes ↓*	yes ↓*	yes ↓*	yes ↓*	yes ↓*
		Z	−2.38	−2.20	−1.34	−1.02	−2.44	−2.43	−3.34
		p-value	0.0017	0.0029	0.025	0.051	0.0014	0.0015	0.0001
		Q (mm/year)	−0.909	−0.418	−0.346	−0.435	−0.975	−0.730	−2.381
		Trend	yes ↓*	yes ↓*	yes ↓*	yes ↓	yes ↓*	yes ↓*	yes ↓*
Spring	Mar-May								
		S_{crt} ($\alpha = 5\%$)	−0.5689	−0.3938	0.3899	−0.2405	−0.4123	0.4623	−1.316
		S_{ITA}	−1.57	−0.96	0.2874	−0.64	−0.08	1.54	−2.19
		$CL_{(1-\alpha)}$	±0.1651	±0.0791	±0.0778	±0.0295	±0.9513	±0.109	±0.883
		Trend	yes ↓*	yes ↓*	yes ↑*	yes ↓*	yes ↓	yes ↑	yes ↓*
		Z	−1.99	−2.00	0.19	−1.03	0.93	0.17	−0.09
		p-value	0.0283	0.005	0.8503	0.0498	0.945	0.4117	0.284
		Q (mm/year)	−1.802	−2.17	0.206	−1.01	1.225	0.312	−0.218
		Trend	yes ↓*	yes ↓*	yes ↑	yes ↓	yes ↑	yes ↑	yes ↓

S_{ITA}, ITA slope indicator; *Z*, M–K trend test statistics; *Q*, Sen's trend slope value.
↑* or ↓* indicates significantly increasing or decreasing trends at 5% level, respectively.

and Zequala stations ($S_{ITA} = -10.35$ mm/year). The summer season rainfall at the Modjo station showed an insignificantly increment rate of 6.49 mm/year at a 5% significance level as the critical slope (S_{crt}) was 1.132 mm/year under the ITA method (Table 5). According to the ITA method, the summer season rainfall trend of Zequla and Modjo stations experienced maximum decrement and increment rates with ITA slope of −10.35 mm/year and +6.49 mm/year, respectively. Based on the M–K test, significant trends were detected for summer rainfall only at Zequala ($Z = -3.25$, $p < 0.05$) and Modjo ($Z = 2.92$, $p < 0.05$) stations.

In the spring season (Belg: March– May), downward trends were dominant, as it occurred in four out of the seven stations (Table 5). It can be seen that the rainfall amount of this season experienced a downward trend except at Koka and Modjo that revealed weak increasing trends with SS values of 1.27 and 1.0 mm/year in that order. During this season, a significant trend was detected only at Aleltu and Bishoftu stations under the M–K test, whereas, in using the ITA method a significant trend was observed in most of the stations except at Koka and Modjo stations which revealed an insignificantly decreasing and increasing trends, respectively (Table 5). Although the rainfall during the spring season is extremely needed for agricultural systems, declining trends of rainfall in this season were dominant in the Modjo catchment. A similar result was also reported in the central highlands of Ethiopia (Rosell 2011), in which our catchment is located, and in the whole country (Gummadi *et al.* 2018).

The trend analysis result shows that the precipitation in winter (Bega: February–December) has a declining trend in all the stations using all the methods (Table 5). Based on the M–K result, the rainfall recorded for the winter season at the Modjo station had the highest statistically significant reduction ($Z = -3.34$, $p = 0.0001$) at the 5% significance level. Moreover, the S_{ITA} value of rainfall during winter was the maximum for the Modjo station ($S_{ITA} = -0.40$ mm/year), which showed a significant decline trend ($S_{crt} = -0.2452$ mm/year), at a 5% level of significance (Table 5). In general, the ITA, M–K , and Sen's slope analysis results of the winter showed more consistency temporal trends as compared to the rainfall trend of the spring and summer seasons. In contrast to our findings, a study conducted in a similar area (Eshetu 2020), reported that there is a non-significant trend in the seasonal rainfall from 1981 to 2010. According to the study, Belg (spring) season rainfall at all the stations experienced an insignificant decline trend over the past 30 years, which is consistence with our findings from the statistical point of view. The same paper also indicated that insignificant trend for the summer (Kiremt) season rainfall in all the stations over the Modjo watershed. However, in our findings, some of the stations (e.g., Modjo) during summer as well as (Aleltu and Bishoftu/Debre zeit) for Belg seasons show significant trends in the period 1981–2020 (Table 5). The inconsistencies between the results may be due to the data length, and quality control approach considered in the current study.

For further visual analysis, the graphical plot of the ITA method is shown in Figures 5–11. Accordingly, no clear trend in summer (JJA) precipitation, except a monotonic increasing trend at Edjere and Modjo stations (Figures 8(c) and 10(c), respectively). The spring season rainfall amount at Aleltu, Edjere, Koka, and Zequala stations showed a clear negative tendency, especially for the high values (Figures 5(c), 8(c), 9(c), and 11(c), respectively). For the other stations, the spring season rainfall revealed a trendless time-series. Negative rainfall trend behavior has been detected in the winter season at

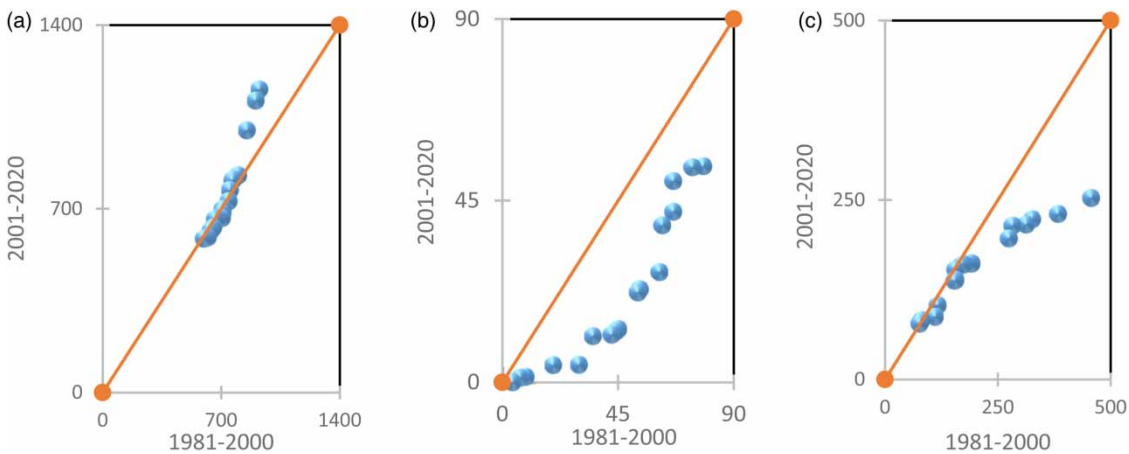

Figure 5 | Graphical plot of the ITA method for the Aleltu station: (a) summer, (b) winter, and (c) spring seasons.

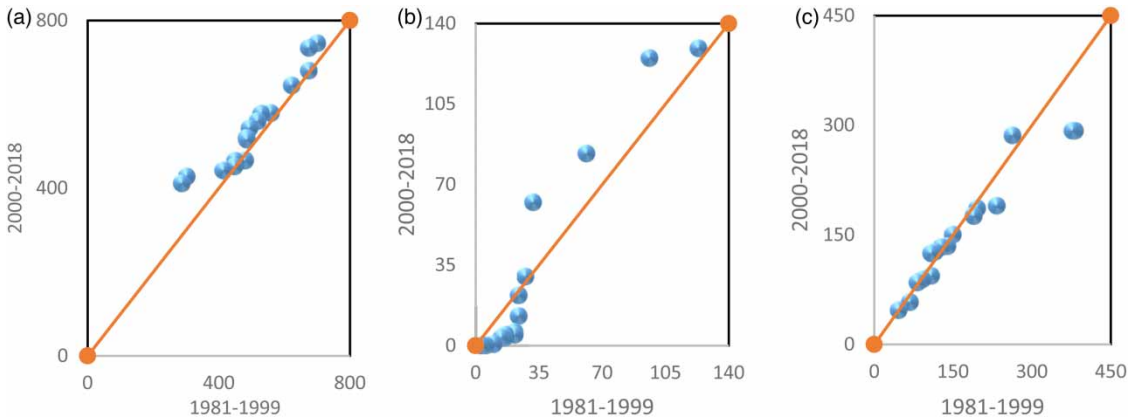

Figure 6 | Graphical plot of the ITA method for the Bishoftu station: (a) summer, (b) winter, and (c) spring seasons.

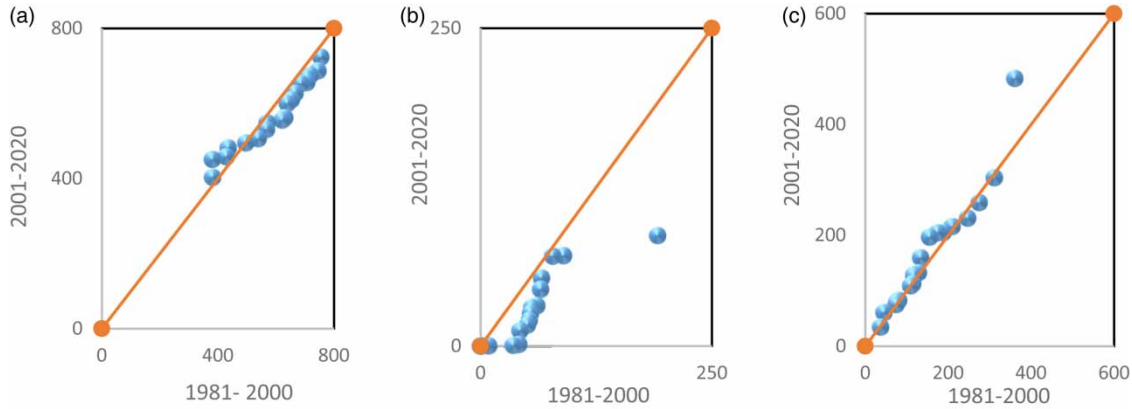

Figure 7 | Graphical plot of the ITA method for the Chefe donsa station: (a) summer, (b) winter, and (c) spring seasons.

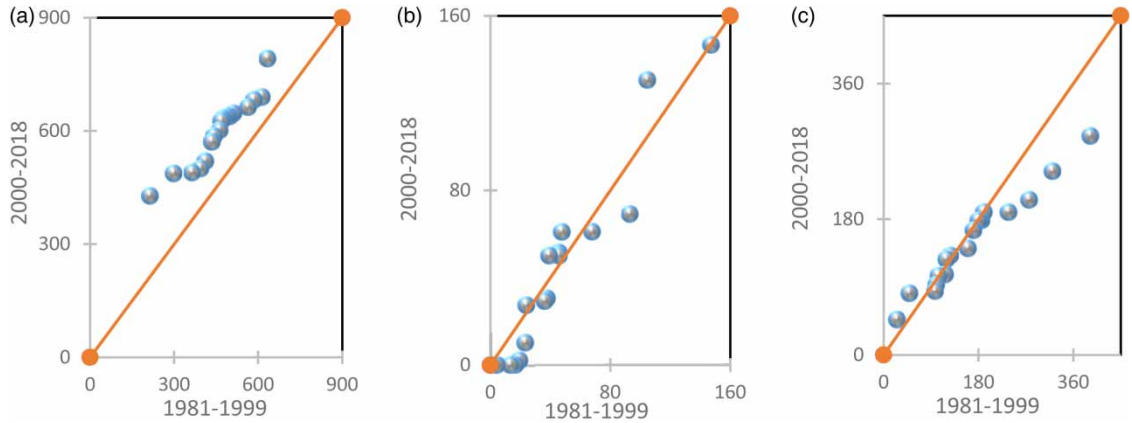

Figure 8 | Graphical plot of the ITA method for the Edjere station: (a) summer, (b) winter, and (c) spring seasons.

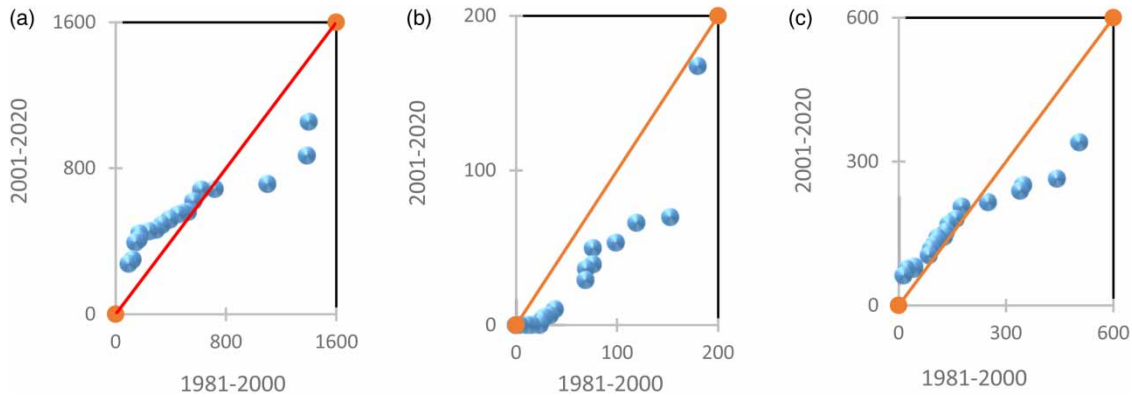

Figure 9 | Graphical plot of the ITA method for the Koka dam station: (a) summer, (b) winter, and (c) spring seasons.

all the stations, while no trends can be clearly identified in summer (Figure 5(a)) and spring seasons (Figure 5(c)) at the Aleltu station. A clear declined trend has been detected in winter rainfall except at Edjere, Bishoftu, and Modjo stations that recorded a trendless time-series of the period. With some exceptions concerning the high rainfall values for winter seasons, no trend was detected in Bishoftu (Figure 6(b)). In this station, summer rainfall points were distributed above the 1:1 line, but with no trend tendency for the medium, and some of the high rainfall values.

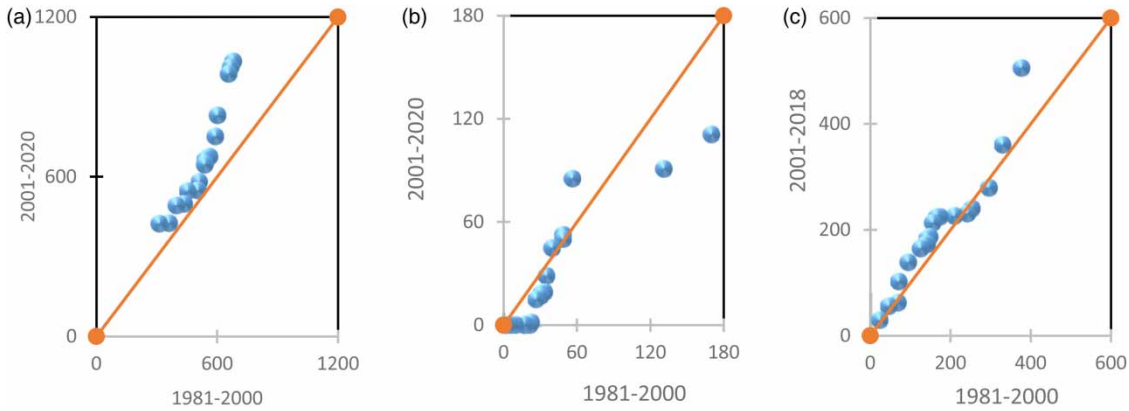

Figure 10 | Graphical plot of the ITA method for the Modjo catchment: (a) summer, (b) winter, and (c) spring seasons.

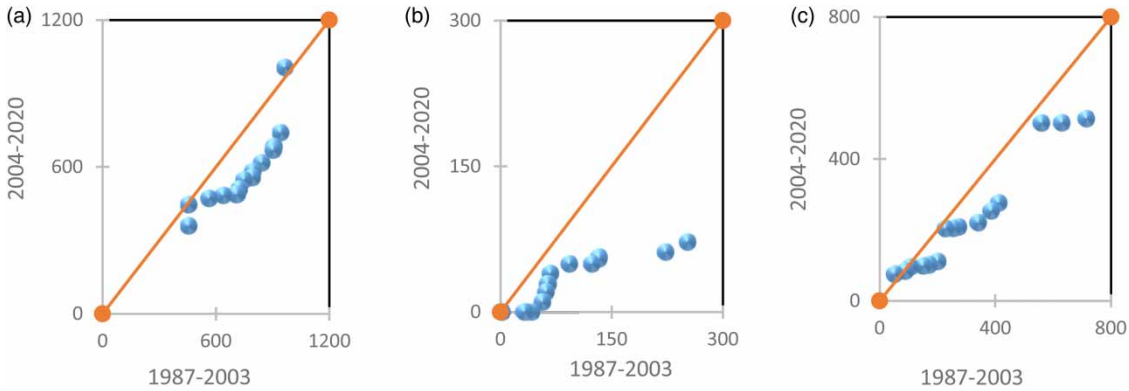

Figure 11 | Graphical plot of the ITA method for the Zequala station: (a) summer, (b) winter, and (c) spring seasons.

According to the plot in Figure 7, except for winter season, no trend was detected at the Chefe donsa station during summer and autumn seasons, because the points are concentrated around the 1:1 line. The rainfall amount of the summer season is with the clearest trend evidence, as all the low, medium, and high values were positioned in the upper triangle at the Chefe donsa station (Figure 7(a)). For the low rainfall values of the winter season negative trend tendencies can be clearly observed for this station (Figure 7(b)). However, a no trend condition was evidenced in autumn at the Chefe donsa station, with few exceptions of the high rainfall values (Figure 7(c)). The plot in Figure 8, except for summer season, no clear trend was identified at the Edjere station during winter and spring seasons. The rainfall amount of the summer season is with the clearest trend evidence, as all the low, medium and high values were positioned in the upper triangle (Figure 8(a)). Except for some high rainfall values during the spring season (Figure 8(c)), no trend tendencies were observed in winter and spring seasons at the Edjere station (Figure 8(b) and 8(c)). There was a negative trend of the high rainfall values of summer, spring and winter rainfall patterns at the Koka station, with the highest values positioned largely far from the 1:1 line (Figure 9). Positive trend has been detected in summer, which is more evident for the low rainfall values. At this station, the lower rainfall values during summer show an inclined trend but the higher values during this season distributed far from the 1:1, and located in the lower triangle (Figure 9(a)). Overall, no trend tendencies were evidenced for the low and medium rainfall values at this station during winter and spring seasons (Figure 9(b) and 9(c), respectively).

Modjo is the station with the clear increased trend tendencies for the high rainfall values in the summer season (Figure 10(a)), with no significant trend evidences for the low and medium rainfall values during winter and spring seasons of the period. At this station, except few high rainfall values, all the low, and medium values were concentrated around the 1:1 line during both winter and spring seasons. Hence, no trend was detected at the Modjo station during the winter and autumn seasons (Figure 10(b) and 10(c), respectively). All the seasons evidenced clear negative trends, with some exceptions

concerning the low rainfall values in summer, winter, and spring seasons at the Zequala station (Figure 11). The findings from the graphical analysis are in line with the statistical estimations under the ITA method (Table 5). In summary, the rainfall trend analysis indicates an inverse relationship between rainfall amount and temporal trend, i.e., the area which received the largest rainfall amounts showed a decreasing trend. For example, the northwestern part of the watershed received the maximum annual rainfall of the study period, but revealed a declining trend.

4.4. Comparison of trend analysis results

The M–K , SS, and ITA methods have been used and compared in this paper. The main intent is to determine accurate trend tendency in time-series data. A comparison of results of the rainfall trends estimated by different tests is summarized in Table 6. Consistent results were found, except in some cases in time-series trend analysis among methods used in the study. Accordingly, significant trends were detected only in one (12.3% of total stations) in annual and in two (28.6%) summer season precipitation using the M–K test, whereas these were two in applying the ITA method (Table 6). At the same time, two (28.6%) and five (71.4%) of the stations for the spring season rainfall amount experienced statistically significant trend using the M–K test and ITA method, respectively, indicates the ITA method displays a more definite significant pattern than the M–K test. On the other hand, the number of significant trend identified by the M–K and ITA tests are six (85.7%) and seven (100%), respectively, for the winter season (Table 6). This indicates, there has been some differences regarding the number of significant trends among the methods used in the study. Therefore, all the statistically significant trends identified by the ITA method were not supported by the classical M–K tests.

In this study, the spatiotemporal trend analysis results indicate the M–K and ITA method have some contradicting results. For example, a statistically increasing trend at Koka during spring rainfall is detected as a statistically decreasing trend under the ITA method (Table 6). Additionally, the statistically insignificant rainfall trends of spring and winter seasons at the Edjere station as well as the insignificantly increasing trend of the Chefe donsa station by the M–K test detected all as statistically significant trends when applying the ITA method (Table 6). Similar contradicting results between the classical M–K test and ITA method were also reported in previous studies. This may be due to data distribution, sample size, and extreme values while using the classical tests (Mekonen & Berlie 2020; Mallick *et al.* 2021). It is important to point out that the ITA method is insensitive to the sample's size, data distribution, and serial autocorrelation effects as evidenced from previous studies (Şen 2012; Machiwal *et al.* 2019). Therefore, as it can be demonstrated graphically on the Cartesian Coordinate System to provide a clear visual display for further clarification, the ITA method is found to be more robust for trend analysis in time-series data than classical methods (Alashan 2020). Furthermore, taking the advantage of its freeness from the assumptions of data normality, serial autocorrelation, its independency from record length as well as a seasonal cycle (Cui *et al.* 2017; Kisi *et al.* 2018; Zhou *et al.* 2018).

4.5. Implications of precipitation changes at catchment scale

4.5.1. Implication on agricultural systems

Adequate precipitation amount is necessary to ensure high and quality yield in the agricultural sector, particularly for the rain-fed agriculture-dependent countries. Among the climate variables, precipitation is the key determinant in the agrarian

Table 6 | Comparison of different trend detection methods in annual and wet season rainfall series

	Annual rainfall		Summer season		Spring season		Winter season	
Stations	**M–K test**	**ITA**	**M–K test**	**ITA**	**M–K test**	**ITA**	**M–K test**	**ITA**
Alelru	↓	↓*	↑	↑	↓*	↓*	↓*	↓*
Bishoftu	↑	↑	↓	↓*	↓*	↓*	↓*	↓*
Chefe donsa	↑	↑	↓	↓	↑	↑*	↓*	↓*
Edjere	↑	↑	↑	↑	↓	↓*	↓	↓*
Koka	↑	↑	↑	↑	↑	↓	↓*	↓*
Modjo	↑	↑	↑*	↑	↑	↑	↓*	↓*
Zequala	↓*	↓*	↓*	↓*	↓	↓*	↓*	↓*

↓* indicates significantly decreasing trend at 5% level; ↑* indicates significantly increasing trend at 5% level; ↑ indicates insignificantly increasing trend; ↓ indicates insignificantly decreasing trend.

counties like Ethiopia. Its spatial and temporal distribution may affect the cropping system, schedule as well as productivity. Changes in this variable are known to be among the foremost long-term threats to humans, with an impact on all sectors of life generally and agriculture in particular (Larbi *et al.* 2022). It is worth noting that the major traditional occupation in the study area remains agriculture which is nearly rain-fed. According to CSA (2014), the influence of agriculture is incomparable that employs about 80% of the labor force and accounts for 45% of the GDP and 85% of the export revenue in any single year over the country. Therefore, any variation in the occurrence and distribution in rainfall amount can significantly affect the agricultural productivity and food security of the region.

The Modjo catchment receives high precipitation amounts under the present condition. More than 60% of total annual rainfall is precipitated during the summer (JJA) season. In most of the stations, rainfall of the major rainy season (summer season) revealed an increasing trend in the considered period. Therefore, sufficiently available rainfall during this season leads to greater moisture availability and facilitates early planting of long-duration crops (Gummadi *et al.* 2018). Spring (MAM) season, contributes around 19% of the annual mean rainfall. However, the catchment exhibits an overall declining trend tendency during this season (Table 5). It is clearly observed that the spring season is the cultivation and growing time for short duration crops. Hence, the rainfall precipitated during this season is extremely important for agricultural activities and productivity in the region. Therefore, decreasing trends in the rainfall amount of March to May months (spring season) will have serious impacts on the production and productivity of agricultural systems in such a highly populated region. It also affects soil moisture availability and disturbs the summer season cropping schedule, in turn, it makes future agricultural activities more challenging in the area.

4.5.2. Implication on water resources availability

Both surface and ground water resources are vital natural sources in the study catchment. Even though most of the rainfall trends did not show significant changes in statistical terms, the general tendency is toward increasing both in the annual and summer season (Tables 4 and 5). For example, 71.4% of the stations showed increasing trends during the summer (JJA) season rainfall amounts (Table 5). Given the strategic importance of the Awash river (in which our study area is located), any change in the spatial and temporal rainfall can impact multiple users including the Capital Addis Ababa. Considering water resource abstraction as constant and insignificant, the increasing trend in the amount of rainfall during this season is expected to increase either surface runoff or ground water recharges.

The increasing trends in the major rainy season may have supported by increased frequency of occurrence and magnitude of extreme events, which will have expected impacts to increase flooding and soil erosion risks. This would also increase the chance of flooding and erosion hazards within the catchment. The two major hydro-meteorological hazards in the Awash river basin are erosion and flooding that affects life and properties every year (Dereje *et al.* 2015). Flooding, on its parts can cause siltation and sedimentation problems, while erosion destroys the fertility of farmlands, and in turn reduced land productivity. In addition, increase of summer rainfall amounts plays a significant role on sediment flows into the Awash river, which can impose sedimentation problems to the downstream Koka hydroelectric reservoir. This has also implied the increasing tendency of siltation risks on the hydroelectric reservoir that can reduce the power generation capability of the dam. Various studies conducted in different parts of the country (e.g., Ayele *et al.* 2016; Matewos & Tefera 2020) averred that changes and fluctuations in hydro-climatic variables significantly affected water resources and food security in the country.

5. CONCLUSION AND IMPLICATIONS

This study was conducted to explore the spatial variability and temporal trends of annual and seasonal precipitation of the Modjo catchment, central Ethiopia. The temporal trends were analyzed using the comparative approach of the classical M–K test and ITA method. In the study, daily rainfall records from seven stations for the period 1981–2020 were used. The results show that the average annual rainfall of the catchment is between 846 and 1,131 mm, with moderate inter-annual variability across the studied stations. Generally, the seasonal rainfall variability was higher than the annual rainfall variability, as evidenced by high CV, which is closely related to its geographical location and complex terrain.

There were no systematic patterns of temporal trends and spatial variations of annual and seasonal rainfall amounts over the study catchment. Increasing trends for the annual rainfall patterns were observed in most of the stations, however, significant trends were detected only at Aleltu and Zequala stations. The summer (JJA) season rainfall showed raising trend in most of the stations, however, statistically significant trend was identified at Bishoftu, Modjo and Zequala stations. The

spring (MAM) season rainfall showed decreasing trend in the studied stations except at Chefe donsa, Koka and Modjo stations. The declined trend of spring rainfall indicating tendencies for increasing of the number of dry days and the reduction of rainfall magnitude of this season in most of the stations. On the other hand, the winter season rainfall revealed statistically significant declined trends in all the stations under all the methods, except at Edjere that showed insignificant decreasing trend under the M–K test.

Spatially, mixed rainfall variability was experienced over the Modjo catchment. It was observed that the annual and seasonal precipitations were unevenly distributed over the area. The annual rainfall distribution of the period decreased from west to east. The northwestern part of the catchment received the highest annual precipitation of the period that ranges from 1,065 to 1,085 mm. Whereas the lowest annual precipitation was observed in the southwestern and southeastern parts, which varies between 950 and 970 mm.

Comparing the results from the two methods, the significant trend in annual rainfall occupies 14.3% in the M–K test and 28.6% in the ITA method, whereas this is, respectively, 28.6 and 71.4% during the spring season, which indicates that more definite significant patterns are displayed by the ITA method than the M–K test. Overall, the ITA method allows more detailed interpretations about trend detection than that of the M–K test. It has also the benefit for identifying hidden trends as well as graphical illustration of the trend variability of extreme events of annual and seasonal rainfall over the classical M–K test.

The rainfall patterns during summer and spring seasons have shown increasing and decreasing tends, which could have implications to accelerate extreme events (such as surface runoff and soil erosion) and low agricultural productivities, respectively. Hence, there is a need for planning of effective adaptation and mitigation strategies at local scale. the involvement of stakeholders together with government organizations is essential in planning efficient strategies in order to minimize the negative impact of climate change in such rain-fed agricultural regions. The river and various small streams are accessible in the catchment. For the production of crops, especially when the Belg season rain declines, implementing small-scale irrigation schemes using such surface as well as groundwater sources will be very important to enhance agricultural productivity. To compensate and effectively utilize the highly variable wet season rainfall, providing short duration crop varieties is recommended in the area. Finally, the study findings have an essential contribution to the detailed trend interpretations as it quantitatively assesses the annual and seasonal trends in the 'low', 'medium', and 'high', values.

ACKNOWLEDGEMENTS

The Ethiopian National Meteorological Service Agency (NMSA) is acknowledged for providing rainfall data used in this study. The authors would like to acknowledge Jimma and Assosa universities for the educational support. We are also pleased to thank the editor and reviewers of the manuscript for their time and constructive comments that we used to improve the quality of this manuscript.

FUNDING

This research did not receive any specific grant from funding agencies in the public, commercial, or not-for profit sectors.

DATA AVAILABILITY STATEMENT

Data cannot be made publicly available; readers should contact the corresponding author for details.

CONFLICT OF INTEREST

The authors declare there is no conflict.

REFERENCES

Agha, O. M., Bagçac, S. C. & Sarlak, N. 2017 Homogeneity analysis of precipitation series in north Iraq. IOSR J. *Appl. Geol. Geophys.* **5** (3), 57–63.

Aieb, A. K., Madani, M., Scarpa, B., Bonaccorso, K. & Lefsih, K. 2019 A new approach for processing climate missing databases applied to daily rainfall data in Soummam watershed, Algeria. *Heliyon* **5** (2), 1247.

Alashan, S. 2018 An improved version of innovative trend analyses. *Arab J. Geosci.* **11** (3), 50. https://doi.org/10.1007/s12517-018-3393-x.

Alashan, S. 2020 Combination of modified Man-Kendall method and Sen innovative trend analysis. *Eng. Rep.* **2** (3), 2–13. https://doi.org/10.1002/eng2.12131.

Alemu, M. M. & Bawoke, G. T. 2019 Analysis of spatial variability and temporal trends of rainfall in the Amhara region, Ethiopia. *J. Water Clim. Change* **11** (4), 1505–1520. https://doi.org/10.2166/wcc.2019.084.

Alifujiang, Y., Abuduwaili, J., Maihemuti, B., Emin, B. & Groll, M. 2020 Innovative trend analysis of precipitation in the Lake Issyk-Kul Basin, Kyrgyzstan. *Atmosphere* **11** (4), 1–16. https://doi.org/10.3390/atmos11040332.

Arragaw, A. & Woldeamlak, B. 2017 Local spatiotemporal variability and trends in rainfall and temperature in the central highlands of Ethiopia. *Geogr. Ann. Ser. A Phys. Geogr.* **99** (2), 85–101. http://doi.org/10.1080/04353676.2017.1289460.

Asfaw, A., Simane, B., Hassen, A. & Bantider, A. 2018 Variability and time-series trend analysis of rainfall and temperature in northcentral Ethiopia: a case study in Woleka sub-basin. *Weather Clim. Extremes* **19**, 29–41. http://doi.org/10.1016/j.wace.2017.12.002.

Ay, M. & Kisi, O. 2015 Investigation of trend analysis of monthly total precipitation by an innovative method. *Theor. Appl. Climatol.* **120**, 617–629.

Ayele, H. S., Li, M. H., Tung, C. P. & Liu, T. M. 2016 Impact of climate change on runoff in the Gilgel Abbay watershed, the upper Blue Nile Basin, Ethiopia. *Water* **8**, 380.

Aziz, O. & Burn, D. H. 2005 Trends and variability in the hydrological regime of the Mackenzie River Basin. *J. Hydrol.* **319**, 282–294. http://doi.org/10.1016/j.jhydrol.2005.06.039.

Bayable, G., Amare, G., Alemu, G. & Gashaw, T. 2021 Spatiotemporal variability and trends of rainfall and its association with Pacific Ocean Sea surface temperature in West Harerge Zone, Eastern Ethiopia. *Environ. Syst. Res.* **10** (7), 1–21. https://doi.org/10.1186/s40068-020-00216-y.

Bekele, D., Alamirew, T., Zeleke, G. & Melese, A. M. 2017 Analysis of rainfall trend and variability for agricultural water management in awash River Basin, Ethiopia. *J. Water Clim. Change* **8** (1), 127–141. https://doi.org/10.2166/wcc.2016.044.

CSA (Central Statistical Agency of Ethiopia) 2014 Agricultural sample survey. Report on area and production of major crops. *Statistical Bulletin* **8**, 578. Addis Ababa, Ethiopia.

Caloiero, T. 2019 Evaluation of rainfall trends in the South Island of New Zealand through the innovative trend analysis (ITA). *Theor. Appl. Climatol.* **139**, 493–504. http://doi.org/10.1007/s00704-019-02988-5.

Caloiero, T., Coscarelli, R. & Ferrari, E. 2018 Application of the innovative trend analysis method for the trend analysis of rainfall anomalies in Southern Italy. *Water Resour. Manage.* **32**, 4971–4983. https://doi.org/10.1007/s11269-018-2117-z.

Cheung, W. H., Senay, G. B. & Singh, A. 2008 Trends and spatial distribution of annual and seasonal rainfall in Ethiopia. *Int. J. Climatol.* **28**, 1723–1734. http://doi.org/10.1002/joc.1623.

Cui, L., Wang, L., Lai, Z., Tian, Q., Liu, W. & Li, J. 2017 Innovative trend analysis of annual and seasonal air temperature and rainfall in the Yangtze River basin, China during 1960–2015. *J. Atmos. Sol. Terr. Phys.* **164**, 48–59. https://doi.org/10.1016/j.jastp.2017.08.001.

Degefu, M. A. & Bewket, W. 2014 Variability and trends in rainfall amount and extreme event indices in the Omo-Ghibe River Basin, Ethiopia. *Reg. Environ. Change* **14** (2), 799–810. https://doi.org/10.1007/s10113-013-0538-z.

Dereje, A., Kansal, M. L. & Sen, S. 2015 Assessment of water scarcity and its impacts on sustainable development in Awash basin, Ethiopia. *Sustainable Water Resour. Manage.* **1**, 71–87.

Eshetu, M. 2020 Hydro-climatic variability and trend analysis of Modjo river watershed, Awash River Basin of Ethiopia. *Hydrol. Current Res.* **11** (2), 1–8.

Fitsum, B., Nega, M. & Dejen, T. 2017 Analysis of current rainfall variability and trends over Bale-Zone, South Eastern highland of Ethiopia. *Clim. Change* **3** (12), 889–902. http://doi.org/10.23959/sfjgw-1000007.

Gebremichael, H. B., Raba, G. A., Beketie, K. T., Feyisa, G. L. & Siyoum, T. 2022 Changes in daily rainfall and temperature extremes of upper Awash Basin, Ethiopia. *Sci. Afr.* **16**, e01173. https://doi.org/10.1016/j.sciaf.2022.e01173.

Gedefaw, M., Wang, H., Yan, D., Song, X., Yan, D., Dong, G., Wang, J., Girma, A., Ali, B. R., Batsuren, D., Abiyu, A. & Qin, T. 2018 Trend analysis of climatic and hydrological variables in the Awash River Basin, Ethiopia. *Water* **10**, 1554. https://doi.org/10.3390/w10111554.

Gummadi, S., Rao, K. P. C., Seid, J., Gizachew, L., Kadiyala, M. D. M., Robel, T., Tilahun, A. & Whitbread, A. 2018 Spatiotemporal variability and trends of precipitation and extreme rainfall events in Ethiopia in 1980-2010. *Theor. Appl. Climatol.* **134**, 1315–1328. https://doi.org/10.1007/s00704-017-2340-1.

Harka, A. E., Jilo, N. B. & Behulu, F. 2021 Spatial-temporal rainfall trend and variability assessment in the Upper Wabe Shebelle River Basin, Ethiopia: application of innovative trend analysis method. *J. Hydrol. Reg. Stud.* **37**, 100915. https://doi.org/10.1016/j.ejrh.2021.100915.

Hussain, F., Nabi, G. & Wu, R. S. 2021 Spatiotemporal rainfall distribution of Soan River Basin, Pothwar Region, Pakistan. *Adv. Meteorol.* **17**, 1–24. https://doi.org/10.1155/2021/6656732.

Jury, M. R. & Funk, C. 2012 Climatic trends over Ethiopia: regional signals and drivers. *Int. J. Climatol.* **33** (8), 1924–1935. https://doi.org/10.1002/joc.3560.

Kendall, M. G. 1975 *Rank Correlation Methods*. Charles Griffin and Co. Ltd, London, UK.

Kisi, O., Santos, C. A. G., Silva, R. M. D. & Zounemat-Kermani, M. 2018 Trend analysis of monthly stream flows using Sen's innovative trend method. *Geofizika* **35** (1), 53–68. https://doi.org/10.15233/gfz.2018.35.3.

Larbi, C., Nyamekye, S. Q., Dotse, D. K., Danso, T., Annor, E., Bessah, E., Limantol, A. M., Attah-Darkwa, T., Kwawuvi, D. & Yomo, M. 2022 Rainfall and temperature projections and the implications on streamflow and evapotranspiration in the near future at the Tano River Basin of Ghana. *Sci. Afr.* **15**, e01071. https://doi.org/10.1016/j.sciaf.2021.e01071.

Li, T. & Luo, J. 2011 Projection of future precipitation change over China with a high-resolution global atmospheric model. *Adv. Atmos. Sci.* **28** (2), 464–476.

Machiwal, D., Gupta, A., Jha, M. K. & Kamble, T. 2019 Analysis of trend in temperature and rainfall time series of an Indian arid region: comparative evaluation of salient techniques. *Theor. Appl. Climatol.* **136** (1–2), 301–320. https://doi.org/10.1007/s00704-018-2487-4.

Mahtsente, T. T., Kumar, L., Koech, R. & Zemadim, B. 2019 Hydro-climatic variability: a characterization and trend study of the Awash River Basin, Ethiopia. *Hydrology* **6**, 1–19.

Malik, A., Kumar, A., Guhathakurta, P. & Kisi, O. 2019 Spatial-temporal trend analysis of seasonal and annual rainfall (1966–2015) using innovative trend analysis method with significance test. *Arab. J. Geosci.* **12** (328), 1–23. https://doi.org/10.1007/s12517-019-4454-5.

Mallick, J., Talukdar, S., Alsubih, M., Salam, R., Ahmed, M., Ben, K. N. & Shamimuz- zaman, M. 2021 Analyzing the trend of rainfall in Asir region of Saudi Arabia using the family of Mann-Kendall tests, innovative trend analysis, and detrended fluctuation analysis. *Theor. Appl. Climatol.* **143** (1–2), 823–841. https://doi.org/10.1007/s00704-020-03448-1.

Mann, H. B. 1945 Nonparametric tests against trend. *J. Econom. Soc.* **13**, 245–259.

Matewos, T. & Tefera, T. 2020 Local level rainfall and temperature variability in drought-prone districts of rural Sidama, central rift valley region of Ethiopia. *J. Phys. Geogr.* **41**, 36–53.

Mekonen, A. A. & Berlie, A. B. 2020 Spatiotemporal variability and trends of rainfall and temperature in the northeastern highlands of Ethiopia. *Model Earth Syst. Environ.* **6** (1), 285–300. https://doi.org/10.1007/s40808-019-00678-9.

Misrak, T. H., Teshale, W. & Menfese, T. 2019 Spatial and temporal climate variability and change in the Bilate catchment, central Rift Valley lakes region, Ethiopia. *Phys. Geogr.* **42** (3), 199–225.

Mohammed, Y., Yimer, F., Tadesse, M. & Tesfaye, K. 2018 Variability and trends of rainfall extreme events in north east highlands of Ethiopia. *Int. J. Hydrol.* **2** (5), 594–605. https://doi.org/10.15406/ijh.2018.02.00131.

Oztopal, A. & Şen, Z. 2017 Innovative trend methodology applications to precipitation records in Turkey. *Water Resour. Manage.* **31** (3), 1–11. https://doi.org/10.1007/s11269-016-1343-5.

Pingale, S. M., Khare, D., Jat, M. K. & Adamowski, J. 2014 Spatial and temporal trends of mean and extreme rainfall and temperature for the 33 urban centers of the arid and semi-arid state of Rajasthan, India. *Atmos. Res.* **138**, 73–90.

Rosell, S. 2011 Regional perspective on rainfall changes and variability in the central highlands of Ethiopia, 1978-2007. *Appl. Geogr.* **31** (1), 329–338. https://doi.org/10.1016/j.apgeog.2010.07.005.

Rosell, S. & Holmer, B. 2007 Rainfall change and its implications for Spring harvest in South Wollo, Ethiopia. *Geogr. Ann.* **89** (4), 287–299.

Seleshi, Y. & Camberlin, P. 2006 Recent changes in dry spell and extreme rainfall events in Ethiopia. *Theor. Appl. Climatol.* **83** (1–4), 181–191.

Şen, P. K. 1968 Estimates of the regression coefficient based on Kendall's tau. *J. Am. Stat. Assoc.* **63** (324), 1379–1389. https://doi.org/10.1080/01621459.1968.10480934.

Şen, Z. 2012 Innovative trend analysis methodology. *J. Hydrol. Eng.* **17**, 1042–1046.

Şen, Z. 2015 Innovative trend significance test and applications. *Theor. Appl. Climatol.* **127**, 939–947.

Şen, Z. 2017 Innovative trend significance test and applications. *Theor. Appl. Climatol.* **127** (3–4), 939–947.

Şişman, E. & Kizilöz, B. 2021 The application of piecewise ITA method in Oxford, 1870–2019. *Theor. Appl. Climatol.* **145**, 1451–1465. https://doi.org/10.1007/s00704-021-03703-z.

Viste, E., Korecha, D. & Sorteberg, A. 2013 Recent drought and precipitation tendencies in Ethiopia. *Theor. Appl. Climatol.* **112** (3–4), 535–551.

Wagesho, N., Goel, N. & Jain, M. 2013 Temporal and spatial variability of annual and seasonal rainfall over Ethiopia. *Hydrol. Sci. J.* **58**, 354–373. https://doi.org/10.1080/02626667.2012.754543.

Worku, G., Teferi, E., Bantider, A. & Yihun, D. 2019 Observed changes in extremes of daily rainfall and temperature in Jemma Sub-Basin, Upper Blue Nile Basin, Ethiopia. *Theor. Appl. Climatol.* **135**, 839–854.

Worku, M., Gudina, L., Kassahun, T. B. & Emmanuel, G. 2022 Rainfall variability and trends in the Borana zone of southern Ethiopia. *J. Water Clim. Change*, 1–20. https://doi.org/10.2166/wcc.2022.173.

Wu, H. & Qian, H. 2017 Innovative trend analysis of annual and seasonal rainfall and extreme values in Shaanxi, China, since the 1950s. *Int. J. Climatol.* **37**, 2582–2592.

Yimer, S. M., Kumar, N., Bouanani, A., Tischbein, B. & Borgemeister, C. 2020 Homogenization of daily time series climatological data in the Eastern Nile basin, Ethiopia. *Theor. Appl. Climatol.* **143**, 737–760.

Yue, S. & Wang, C. Y. 2002 Applicability of pre-whitening to eliminate the influence of serial correlation on the Mann-Kendall test. *Water Resource Res.* **38** (6), 1068. https://doi.org/10.1029/2001WR000861.

Zhou, Z., Wang, L., Lin, A., Zhang, M. & Niu, Z. 2018 Innovative trend analysis of solar radiation in China during 1962–2015. *Renewable Energy* **119**, 675–689. https://doi.org/10.1016/j.renene.2017.12.052.

First received 26 June 2022; accepted in revised form 2 October 2022. Available online 14 October 2022